Composition of Supported Model Membranes Determined by Neutron Reflection

Hanna P. Vacklin,*,† Fredrik Tiberg,‡ Giovanna Fragneto,§ and Robert K. Thomas†

Physical and Theoretical Chemistry Laboratory, Oxford University, South Parks Road, Oxford OX1 3QZ, United Kingdom, Camurus AB, Ltd., Ideon Science Park, Gamma 2, SE-223 70 Lund, Sweden, and Institut Laue-Langevin, 6 rue Jules Horowitz, BP 156, 38042 Grenoble, France

Received October 22, 2004. In Final Form: January 7, 2005

We have investigated the formation of supported bilayers by coadsorption of dipalmitoyl phosphatidylcholine (DPPC) with the nonionic surfactant β-D-dodecyl maltoside. The adsorption of mixed phospholipid−surfactant micelles on hydrophilic silica surfaces at 25 °C was followed as a function of bulk concentration by neutron reflection. Using chain-deuterated d_{25}-β-D-dodecyl maltoside and d_{62}-DPPC, we demonstrate that it is possible to determine the composition of the bilayers at each stage of a sequential dilution process, which enriches the adsorbed layer in phospholipid and leads to complete elimination of the surfactant. The final supported bilayers have thicknesses of 51 ± 3 Å and are stable to heating to 37 °C once all surfactant has been removed, and the structures agree well with other published data on DPPC supported bilayers. The coadsorption of cholesterol in a DPPC−surfactant mixture was also achieved, and the location and volume fraction of cholesterol in the DPPC bilayer was determined. Cholesterol is located in a 18 ± 1 Å thick layer below the lipid headgroup region and leads to an increased bilayer thickness of 58 ± 2 Å at 26 mol % of cholesterol.

1. Introduction

The formation of phospholipid bilayers to be used as models of biological membranes is a key issue in studies of molecular interactions at biological interfaces. Accurate determination of membrane composition is an essential prerequisite in controlling membrane properties and understanding how they influence the interactions with interfacially active biomolecules. A recently developed method of adsorption from micellar solutions allows a rapid deposition of high-quality phospholipid bilayers on solid supports using the nonionic surfactant β-D-dodecyl maltoside as a solubilizing agent.[1] This method has the interesting potential to be able to incorporate by very simple means defined proportions of other components into the supported phospholipid bilayer. We have followed the formation of dipalmitoyl phosphatidylcholine (DPPC)−surfactant−cholesterol bilayers using neutron reflection and have determined the composition and structure of the bilayers using isotopic labeling of the phospholipid and surfactant in turn.

Single supported bilayers[2] are useful membrane models due to their physical properties and simple geometry, but their formation is not necessarily simple. In addition to solvent evaporation,[3] stacks of bilayers can be spin-coated onto solid supports and have been investigated by neutron and X-ray reflection,[4,5] but inter-bilayer interactions in the stacked structure may interfere with protein adsorption experiments. Langmuir−Blodgett deposition and adsorption of vesicles on solid surfaces[6] can both produce single bilayers. Langmuir monolayers[7−9] can be formed from practically all insoluble amphiphiles, but their successful transfer onto a solid surface requires the monolayer to be in a condensed state, while deposition of fluid bilayers leads to incomplete surface coverage.[10] Langmuir−Shaeffer deposition[11] has been shown to lead to floating bilayers that are more mobile than a bilayer directly adsorbed to a solid surface,[12] but the method still suffers from the same limitations as Langmuir−Blodgett deposition.

Direct adsorption from solution has the advantage over various dipping and coating methods that it is achieved by a simple exchange of liquids and can be easily automated, essential for applications which require simultaneous handling and analysis of multiple samples

* To whom correspondence should be addressed.
† Oxford University.
‡ Camurus AB, Ltd.
§ Institut Laue-Langevin.

(1) Tiberg, F.; Harwigsson, I.; Malmsten, M. Formation of model lipid bilayers at the silica-water interface by co-adsorption with non-ionic dodecyl maltoside surfactant. *Eur. Biophys. J. Biophys. Lett.* **2000**, *29*, 196−203.
(2) Sackmann, E. Supported Membranes: Scientific and Practical Applications. *Science* **1996**, *271*, 43−48.
(3) Seul, M.; Sammon, M. J. Preparation of Surfactant Multilayer Films on Solid Substrates by Deposition from Organic Solution. *Thin Solid Films* **1990**, *185*, 287−305.
(4) Mennicke, U.; Salditt, T. Preparation of solid-supported lipid bilayers by spin-coating. *Langmuir* **2002**, *18*, 8172−8177.
(5) Salditt, T.; Li, C.; Spaar, A.; Mennicke, U. X-ray reflectivity of solid-supported, multilamellar membranes. *Eur. Phys. J. E* **2002**, *7*, 105−116.
(6) Kalb, E.; Frey, S.; Tamm, L. K. Formation of Supported Planar Bilayers by Fusion of Vesicles to Supported Phospholipid Monolayers. *Biochim. Biophys. Acta* **1992**, *1103*, 307−316.
(7) Helm, C. A.; Mohwald, H.; Kjaer, K.; Als-Nielsen, J. Phospholipid Monolayers between Fluid and Solid States. *Biophys. J.* **1987**, *52*, 381−390.
(8) Knobler, C. M. Recent Developments in the Study of Monolayers at the Air-Water-Interface. *Adv. Chem. Phys.* **1990**, *77*, 397−449.
(9) Mohwald, H. Phospholipid and Phospholipid-Protein Monolayers at the Air/Water Interface. *Annu. Rev. Phys. Chem.* **1990**, *41*, 441−476.
(10) Dufrene, Y. F.; Lee, G. U. Advances in the characterization of supported lipid films with the atomic force microscope. *Biochim. Biophys. Acta* **2000**, *1509*, 14−41.
(11) Tamm, L. K.; McConnell, H. M. Supported Phospholipid-Bilayers. *Biophys. J.* **1985**, *47*, 105−113.
(12) Fragneto-Cusani, G. Neutron reflectivity at the solid/liquid interface: examples of applications in biophysics. *J. Phys.: Condens. Matter* **2001**, *13*, 4973−4989.

10.1021/la047389e CCC: $30.25
Published on Web 00/00/0000 PAGE EST: 10.3

with minimum user intervention. Adsorption of vesicles allows the deposition of bilayers on hydrophilic surfaces or of monolayers on hydrophobic surfaces, but the results vary, with adsorption of intact vesicles[13] sometimes accompanying bilayer formation. It has been shown by neutron reflection that bilayers with 70−80% lipid surface coverage can be achieved by this method,[14] with defects (holes, double bilayer islands) uniformly distributed over the surface.[15] Although solid-supported bilayers have also been used as substrates in neutron reflectivity studies of polymer cushions[16,17] and membrane peptides,[18,19] in all cases the models used for data fitting have focused on estimating the surface coverage and layer thickness, not the composition. In this paper we aim to show, via the use of a simple surfactant−phospholipid mixture, that contrast variation can be used to determine the lipid composition of a model membrane. The method of deuterating each component in turn in a binary mixture is well-known in surfactant science and has been extensively used in studies of surfactant adsorption and mixing at the silica−water interface.[20−22]

We have already shown that the adsorption of mixed micelles of *n*-β-D-dodecyl maltoside (DDM) and dioleoyl phosphatidylcholine (DOPC) or 1,2-palmitoyl-oleoyl phosphatidylcholine (POPC) leads to the successful formation of well-defined bilayers with characteristics similar to the bulk lamellar structures of DOPC and POPC.[23] In short, dilution of a mixed micellar bulk solution leads to an exchange between surface and bulk aggregates in a manner that enriches the bilayer in the insoluble lipid. By monitoring the bilayer composition throughout adsorption and rinsing, we have established a procedure that leads to the complete elimination of the surfactant, while variation of the concentrations in the bulk gives some freedom of choice for the surface coverage of the phospholipid. In the present work we concentrate on the adsorption of DPPC, which is commercially available in fully and partially deuterated forms, and aim to demonstrate the compositional resolution of neutron reflection in characterizing phospholipid−surfactant mixtures at the solid−water interface. Although DPPC is below its chain melting temperature at 25 °C, it rapidly coadsorbs from surfactant micelles to form high-quality bilayers, from which all surfactant can be removed by rinsing, after which the bilayers are stable to heating to physiologically relevant temperatures. Because of the availability of several deuterated isotopes, DPPC bilayers can be used to investigate the effect of added components on the resulting bilayer structure. In this case we investigated the coadsorption of cholesterol with DPPC to determine its location and the bilayer composition.

2. Neutron Reflection

Neutron reflection[24−26] measures the structure and composition of an adsorbed layer along the direction perpendicular to the interface, and experiments are routinely performed at air−liquid, solid−liquid, and solid−gas interfaces.[27,28] Although it has been used extensively to study the adsorption of surfactants[29−34] and polymers,[35−37] the use of neutron methods in biological systems[12,38−46] has generally been limited by the necessity of deuteration to achieve the desired resolution. Extensive

(13) Csucs, G.; Ramsden, J. J. Interaction of phospholipid vesicles with smooth metal-oxide surfaces. *Biochim. Biophys. Acta* **1998**, *1369*, 61−70.

(14) Johnson, S. J.; Bayerl, T. M.; McDermott, D. C.; Adam, G. W.; Rennie, A. R.; Thomas, R. K.; Sackmann, E. Structure of an Adsorbed Dimyristoylphosphatidylcholine Bilayer Measured with Specular Reflection of Neutrons. *Biophys. J.* **1991**, *59*, 289−294.

(15) Koenig, B. W.; Kruger, S.; Orts, W. J.; Majkrzak, C. F.; Berk, N. F.; Silverton, J. V.; Gawrisch, K. Neutron reflectivity and atomic force microscopy studies of a lipid bilayer in water adsorbed to the surface of a silicon single crystal. *Langmuir* **1996**, *12*, 1343−1350.

(16) Majewski, J.; Wong, J. Y.; Park, C. K.; Seitz, M.; Israelachvili, J. N.; Smith, G. S. Structural Studies of Polymer-Cushioned Lipid Bilayers. *Biophys. J.* **1998**, *75*, 2363−2367.

(17) Wong, J. Y.; Majewski, J.; Seitz, M.; Park, C. K.; Israelachvili, J. N.; Smith, G. S. Polymer-Cushioned Bilayers. I. A Structural Study of Various Preparation Methods Using Neutron Reflectometry. *Biophys. J.* **1999**, *77*, 1445−1457.

(18) Fragneto, G.; Graner, F.; Charitat, T.; Dubos, P.; Bellet-Amalric, E. Interaction of the third helix of Antennapedia homeodomain with a deposited phospholipid bilayer: A neutron reflectivity structural study. *Langmuir* **2000**, *16*, 4581−4588.

(19) Krueger, S. Neutron reflection from interfaces with biological and biomimetic materials. *Curr. Opin. Colloid Interface Sci.* **2001**, *6*, 111−117.

(20) Penfold, J.; Staples, E.; Tucker, I.; Thomas, R. K. Adsorption of mixed anionic and nonionic surfactants at the hydrophilic silicon surface. *Langmuir* **2002**, *18*, 5755−5760.

(21) Penfold, J.; Staples, E. J.; Tucker, I.; Thompson, L. J.; Thomas, R. K. The structure and composition of mixed cationic and non-ionic surfactant layers adsorbed at the hydrophilic silicon surface. *Physica B* **1998**, *248*, 223−228.

(22) Penfold, J.; Thomas, R. K.; Simister, E.; Lee, E.; Rennie, A. The Structure of Mixed Surfactant Monolayers at the Air-Liquid Interface, as Studied by Specular Neutron Reflection. *J. Phys.: Condens. Matter* **1990**, *2*, SA411−SA416.

(23) Vacklin, H.; Tiberg, F.; Fragneto, G.; Thomas, R. K. Formation of supported phospholipid bilayers via co-adsorption with β-D-dodecyl maltoside. *Biophys. Biochim. Acta* **2005**, *1668*, 17−24.

(24) Bradley, J. E.; Lee, E. M.; Thomas, R. K.; Willatt, A. J.; Penfold, J.; Ward, R. C.; Gregory, D. P.; Waschkowski, W. Adsorption at the Liquid Surface Studied by Means of Specular Reflection of Neutrons. *Langmuir* **1988**, *4*, 821−826.

(25) Hayter, J. B.; Highfield, R. R.; Pullman, B. J.; Thomas, R. K.; McMullen, A. I.; Penfold, J. Critical Reflection of Neutrons − a New Technique for Investigating Interfacial Phenomena. *J. Chem. Soc., Faraday Trans. I* **1981**, *77*, 1437−1448.

(26) Highfield, R. R.; Thomas, R. K.; Cummins, P. G.; Gregory, D. P.; Mingins, J.; Hayter, J. B.; Scharpf, O. Critical Reflection of Neutrons from Langmuir-Blodgett Films on Glass. *Thin Solid Films* **1983**, *99*, 165−172.

(27) Lu, J. R.; Thomas, R. K. Neutron reflection from wet interfaces. *J. Chem. Soc., Faraday Trans.* **1998**, *94*, 995−1018.

(28) Thomas, R. K. Neutron reflection from surfactants adsorbed at the solid/liquid interface. *Prog. Colloid Polym. Sci.* **1997**, *103*, 216−225.

(29) Cummins, P. G.; Penfold, J.; Thomas, R. K.; Simister, E.; Staples, E. The Structure of Mixed Surfactants Adsorbed at the Air Liquid Interface, as Studied by Specular Neutron Reflection. *Physica B* **1992**, *180*, 483−484.

(30) Hines, J. D.; Thomas, R. K.; Garrett, P. R.; Rennie, G. K. Investigation of mixing in binary surfactant solutions by surface tension and neutron reflection: Strongly interacting anionic/zwitterionic mixtures. *J. Phys. Chem. B* **1998**, *102*, 8834−8846.

(31) Hines, J. D.; Thomas, R. K.; Garrett, P. R.; Rennie, G. K.; Penfold, J. Investigation of mixing in binary surfactant solutions by surface tension and neutron reflection: Anionic/nonionic and zwitterionic/nonionic mixtures. *J. Phys. Chem. B* **1997**, *101*, 9215−9223.

(32) Lu, J. R.; Simister, E. A.; Lee, E. M.; Thomas, R. K.; Rennie, A. R.; Penfold, J. Direct Determination by Neutron Reflection of the Penetration of Water into Surfactant Layers at the Air/Water Interface. *Langmuir* **1992**, *8*, 1837−1844.

(33) McDermott, D. C.; Kanelleas, D.; Thomas, R. K.; Rennie, A. R.; Satija, S. K.; Majkrzak, C. F. Study of the Adsorption from Aqueous Solution of Mixtures of Nonionic and Cationic Surfactants on Crystalline Quartz Using the Technique of Neutron Reflection. *Langmuir* **1993**, *9*, 2404−2407.

(34) Penfold, J.; Staples, E.; Cummins, P.; Tucker, I.; Thomas, R. K.; Simister, E. A.; Lu, J. R. Structure of the mixed cationic-non-ionic surfactant monolayer of hexadecyltrimethylammonium bromide and monododecyl hexaethylene glycol at the air/water interface. *J. Chem. Soc., Faraday Trans.* **1996**, *92*, 1549−1554.

(35) Lee, E. M.; Thomas, R. K.; Rennie, A. R. Reflection of Neutrons from a Polymer Layer Adsorbed at the Quartz-Water Interface. *Europhys. Lett.* **1990**, *13*, 135−141.

(36) Purcell, I. P.; Thomas, R. K.; Penfold, J.; Howe, A. M. Adsorption of Sds and Pvp at the Air-Water-Interface. *Colloids Surf., A* **1995**, *94*, 125−130.

(37) Thomas, R. K.; McDermott, D. C.; Fragneto, G. Neutron Reflection from Surfactants and Polymers Adsorbed at the Solid-Liquid Interface. *Abstr. Pap. Am. Chem. Soc.* **1995**, *210*, 193-COLL.

(38) Fragneto, G.; Su, T. J.; Lu, J. R.; Thomas, R. K.; Rennie, A. R. Adsorption of proteins from aqueous solutions on hydrophobic surfaces studied by neutron reflection. *Phys. Chem. Chem. Phys.* **2000**, *2*, 5214−5221.

neutron reflectivity studies of surfactant mixtures at the air−water interface[30,31,34,47] and at the solid−liquid interface[20,21] have been published. Phospholipid monolayers and phospholipid−surfactant interactions have been investigated at the air−water interface using neutron reflection,[48−50] as well as phospholipid−protein interactions.[51,52] More recently, several reflectivity studies of solid-supported bilayers have been reported, including bilayers obtained by deposition of Langmuir monolayers[18,53] and adsorption of lipid vesicles.[15,19]

In this paper, we outline a simple method for determining mixed bilayer composition at the silica−water interface, using contrast variation methods traditionally employed in the study of nonbiological materials. Furthermore, we can show that a perdeuterated phospholipid bilayer at the silica−D_2O interface is a remarkably sensitive environment for quantifying the presence and location of small amounts of other membrane components such as cholesterol.

The sensitivity of neutron reflection to the layer structure depends on the contrast in neutron refractive indices of the components of the layer and the surrounding bulk media. The neutron refractive index depends on the nuclear composition of a material and, thus, may be changed by isotopic substitution of deuterium for hydrogen. The composition is related to the neutron refractive index in two steps. First, a neutron scattering length density ρ is defined as in eq 1,

$$\rho = \sum_j N_j b_j \tag{1}$$

where b_j is the coherent neutron scattering length of nucleus j and N_j is the number density of the nuclei. ρ can be directly calculated from the nuclear composition if the density of a material is known. The neutron refractive index n is related to the scattering length density by eq 2

$$n = 1 - \frac{\lambda^2}{2\pi}\rho \tag{2}$$

where λ is the neutron wavelength. The reflection and transmission of neutrons are described by the Fresnel coefficients r and t, defined in eqs 3 and 4

$$r = \frac{q_1 - q_2}{q_1 + q_2} = \frac{n_1 \sin\theta_1 - n_2 \sin\theta_2}{n_1 \sin\theta_2 + n_2 \sin\theta_2} \tag{3}$$

$$t = \frac{2q_1}{q_1 + q_2} = \frac{2n_1 \sin\theta_1}{n_1 \sin\theta_1 + n_2 \sin\theta_2} \tag{4}$$

where $\theta_1$and θ_2 are the grazing angles and q_1 and q_2 are the momentum transfer vectors of reflection and refraction, respectively, given by eq 5.

$$q_i = \frac{4\pi \sin\theta_i}{\lambda} \tag{5}$$

The reflectivity from a single interface is simply given by the square modulus of the Fresnel reflection coefficient:

$$R = |r|^2 \tag{6}$$

When a thin film is adsorbed at the interface between two bulk media, interference arises between the waves reflected from the upper and lower film boundaries, described by the phase thickness β:

$$\beta = \frac{2\pi}{\lambda} n\tau \sin\theta \tag{7}$$

where τ and n are the thickness and refractive index of the film and θ is the angle of incidence.

The two quantities actually measured in a neutron reflectivity experiment are the film thickness and its refractive index, that is, the scattering length density. Using the Fresnel relations, it is possible to calculate the exact reflectivity from any planar interface between two media of uniform scattering length density. At real interfaces and in particular in adsorbed films, the scattering length density profile is often nonuniform, and it may be necessary to divide the interfacial region into several distinct layers for the purposes of modeling, achieved through the use of the well-known optical matrix method.[54] We have used the Abeles version of the optical matrix method, in which it is assumed that the adsorbed film can be divided into n distinct layers, with each layer assigned a matrix $\mathbf{M}_j$,

(39) Fragneto, G.; Thomas, R. K.; Rennie, A. R.; Penfold, J. Neutron Reflection Study of Bovine Beta-Casein Adsorbed on Ots Self-Assembled Monolayers. *Science* **1995**, *267*, 657−660.
(40) Lu, J. R.; Su, T. J.; Thomas, R. K. Binding of surfactants onto preadsorbed layers of bovine serum albumin at the silica−water interface. *J. Phys. Chem. B* **1998**, *102*, 10307−10315.
(41) Lu, J. R.; Su, T. J.; Thomas, R. K.; Penfold, J.; Webster, J. Structural conformation of lysozyme layers at the air/water interface studied by neutron reflection. *J. Chem. Soc., Faraday Trans.* **1998**, *94*, 3279−3287.
(42) Nylander, T.; Tiberg, F.; Su, T. J.; Lu, J. R.; Thomas, R. K. beta-Casein adsorption at the hydrophobized silicon oxide−aqueous solution interface and the effect of added electrolyte. *Biomacromolecules* **2001**, *2*, 278−287.
(43) Su, T. J.; Lu, J. R.; Thomas, R. K.; Cui, Z. F. Effect of pH on the adsorption of bovine serum albumin at the silica water interface studied by neutron reflection. *J. Phys. Chem. B* **1999**, *103*, 3727−3736.
(44) Su, T. J.; Lu, J. R.; Thomas, R. K.; Cui, Z. F.; Penfold, J. The conformational structure of bovine serum albumin layers adsorbed at the silica−water interface. *J. Phys. Chem. B* **1998**, *102*, 8100−8108.
(45) Su, T. J.; Lu, J. R.; Thomas, R. K.; Cui, Z. F.; Penfold, J. The adsorption of lysozyme at the silica−water interface: A neutron reflection study. *J. Colloid Interface Sci.* **1998**, *203*, 419−429.
(46) Tiberg, F.; Nylander, T.; Su, T. J.; Lu, J. R.; Thomas, R. K. Beta-casein adsorption at the silicon oxide−aqueous solution interface. *Biomacromolecules* **2001**, *2*, 844−850.
(47) Penfold, J.; Staples, E.; Cummins, P.; Tucker, I.; Thompson, L.; Thomas, R. K.; Simister, E. A.; Lu, J. R. Adsorption of mixed cationic-non-ionic surfactants at the air/water interface. *J. Chem. Soc., Faraday Trans.* **1996**, *92*, 1773−1779.
(48) Brumm, T.; Naumann, C.; Sackmann, E.; Rennie, A. R.; Thomas, R. K.; Kanellas, D.; Penfold, J.; Bayerl, T. M. Conformational-Changes of the Lecithin Headgroup in Monolayers at the Air/Water Interface − a Neutron Reflection Study. *Eur. Biophys. J. Biophys. Lett.* **1994**, *23*, 289−295.
(49) Naumann, C.; Brumm, T.; Rennie, A. R.; Penfold, J.; Bayerl, T. M. Hydration of Dppc Monolayers at the Air/Water Interface and Its Modulation by the Nonionic Surfactant C(12)E(4)—a Neutron Reflection Study. *Langmuir* **1995**, *11*, 3948−3952.
(50) Naumann, C.; Dietrich, C.; Lu, J. R.; Thomas, R. K.; Rennie, A. R.; Penfold, J.; Bayerl, T. M. Structure of Mixed Monolayers of Dipalmitoylglycerophosphocholine and Polyethylene Glycol Monododecyl Ether at the Air/Water Interface Determined by Neutron Reflection and Film Balance Techniques. *Langmuir* **1994**, *10*, 1919−1925.
(51) Johnson, S. J.; Bayerl, T. M.; Wo, W. H.; Noack, H.; Penfold, J.; Thomas, R. K.; Kanellas, D.; Rennie, A. R.; Sackmann, E. Coupling of Spectrin and Polylysine to Phospholipid Monolayers Studied by Specular Reflection of Neutrons. *Biophys. J.* **1991**, *60*, 1017−1025.
(52) Naumann, C.; Dietrich, C.; Behrisch, A.; Bayerl, T.; Schleicher, M.; Bucknall, D.; Sackmann, E. Hisactophilin-mediated binding of actin to lipid lamellae: A neutron reflectivity study of protein membrane coupling. *Biophys. J.* **1996**, *71*, 811−823.
(53) Fragneto, G.; Charitat, T.; Bellet-Amalric, E.; Cubitt, R.; Graner, F. Swelling of phospholipid floating bilayers: The effect of chain length. *Langmuir* **2003**, *19*, 7695−7702.
(54) Heavens, O. S. *Optical properties of Thin Films*; Butterworths: London, 1955.

$$[\mathbf{M}_j] = \begin{bmatrix} e^{i\beta_{(j-1)}} & r_j e^{i\beta_{(j-1)}} \\ r_j e^{-i\beta_{(j-1)}} & e^{-i\beta_{(j-1)}} \end{bmatrix} \quad (8)$$

where the quantities r_j, n_j, and β_j are the reflection coefficient, refractive index, and phase thickness of the jth layer. The reflectivity of each layer is given by

$$R = \frac{m_{21}m_{21}^*}{m_{11}m_{11}^*} = |r_j|^2 \quad (9)$$

where m_{ij} and m_{ij}^* are the complex conjugate elements of the matrix $\mathbf{M}$. The total reflectivity from n adsorbed layers is the product of matrices $\mathbf{M}_j$:

$$[\mathbf{M}] = \prod_{j=1}^{n} [\mathbf{M}_j] \quad (10)$$

Interfacial roughness is incorporated in the Abeles model by using a modified reflection coefficient r_j^+:

$$r_j^+ = r_j e^{-(1/2)q_j^2\sigma_j^2} \quad (11)$$

where σ_j is the mean interfacial roughness, q_j is the momentum transfer, and the exponential term describes the interdigitation of the layers j and $j + 1$, that is, the smearing out of a defined step in the scattering length at the interface. The calculation of the reflectivity profile is exact for any given model, no matter how many sublayers the interface is divided into.

3. Data Analysis

The composition of an adsorbed layer is obtained directly from the measured scattering length density (as defined in eq 1), and the layer thickness is related to the position of interference fringes in the reflectivity profile. The resolution of the reflection method is intrinsically quite low (~10 Å), but it can be increased by the use of contrast variation,[55] that is, alteration of the scattering length density profile via deuteration of the solvent and/or film. The optical matrix method[54] was used for fitting data in the AFit (v. 3.1) program,[56] which allows the simulation of reflectivity profiles for layered interfaces by characterizing each layer by its thickness, scattering length density, solvent volume fraction, and roughness. The accuracy of the model is improved by simultaneous fitting of reflectivity profiles of the same system in different contrasts. For example, if the reflectivity of (i) deuterated surfactant and phospholipid in D_2O is compared with that from (ii) deuterated phospholipid and surfactant in D_2O, they should conform to the same physical structure provided that the bilayer formation is reproducible. This way, the overall layer thickness and hydration should be the same in both cases, but each measurement gives the surface excess of the hydrogenous component, that is, phospholipid in case i and surfactant in case ii. If both phospholipid and surfactant are deuterated, reflectivity in a D_2O contrast will arise almost entirely from any hydrogenous additive, for example, cholesterol, and hence, the measurement can be made sensitive to changes as small as ±2 vol % of cholesterol in the bilayer.

For the maximum effectiveness in picturing the different components of the bilayer, estimates of the different molecular scattering length densities are required. It must be emphasized that this is not strictly part of the fitting process, but it makes it possible to decompose the observed scattering length density profiles into molecular volume fractions, which greatly assists the molecular interpretation of the reflectivity. We used volume fractions from molecular dynamics simulations of DPPC bilayers.[57] These have been shown to agree well with experimental data at 50 °C.[58−61] For DDM and cholesterol, specific volumes based on their bulk densities (as quoted for 20 °C by Sigma-Aldrich) were used to calculate the molecular volumes. The estimated component volumes and scattering length densities are shown in Table 1. Although the average volume of the hydrocarbon chains of DPPC in the bulk L_β phase at 20 °C is 804 ± 12 Å^3,[62] we based our modeling on the assumption that the hydrocarbon chain packing is unlikely to be fully crystalline in a situation where there is also an interaction with the polar silica surface and used a value of 890 Å^3, which more closely resembles a disordered liquid crystalline arrangement. At this chain volume, assuming that the acyl carbons are a part of the headgroup region, the all-trans chain length would be 7 × 2.54 Å = 17.8 Å, giving rise to an area per molecule of 50 Å^2. As stated above this estimation of scattering length densities is a device to assist interpretation and can be used to guide data fitting while maintaining the bilayer stoichiometry. What are actually fitted in the procedure described below are the total scattering length density, thickness, and roughness of each layer in the model. Hence, although the decomposition of the scattering length density profile into a distribution of molecular fragments relies on an arbitrary division between headgroup and chain volumes, it has no effect on the absolute values obtained for the scattering length density and thickness.

Table 1. Molecular Volumes (V) and Scattering Length Densities (ρ) Used in Data Fitting[81,82]

	h-DPPC	d_{62}-DPPC	cholesterol	h-DDM	d_{25}-DDM
V/Å^3	1215.8	1215.8	601.7	848.4	848.4
ρ/10^{-6} Å^{-2}	0.23	6.97	0.22	0.60	3.67
$V_{headgroup}$/Å^3	326.3	326.3		497.4	497.4
$\rho_{headgroup}$/ 10^{-6} Å^{-2}	1.84	1.84		1.31	1.31
V_{chains}/Å^3	889.2	889.2		351.0	351.0
ρ_{chains}/ 10^{-6} Å^{-2}	−0.37	6.89		−0.39	7.02

In the case of a mixed layer of two components, the resultant scattering length density will be a sum of the molecular scattering length densities weighted by the volume fractions of each component and any solvent present in the layer. For example, in a mixture of two components, A and B, the scattering length density will be

(55) Crowley, T. L.; Lee, E. M.; Simister, E. A.; Thomas, R. K. The Use of Contrast Variation in the Specular Reflection of Neutrons from Interfaces. *Physica B* **1991**, *173*, 143−156.

(56) Thirtle, P. N. *AFit simulation program*; University of Oxford: Oxford, 1997 (http://physchem.ox.ac.uk/~rkt/links/software).

(57) Armen, R. S.; Uitto, O. D.; Feller, S. E. Phospholipid component volumes: Determination and application to bilayer structure calculations. *Biophys. J.* **1998**, *75*, 734−744.

(58) Wiener, M. C.; White, S. H. Structure of a Fluid Dioleoylphosphatidylcholine Bilayer Determined by Joint Refinement of X-Ray and Neutron-Diffraction Data. 3. Complete Structure. *Biophys. J.* **1992**, *61*, 434−447.

(59) Small, D. M. *The Physics and Chemistry of Lipids*; Plenum Press: New York, 1986.

(60) Costigan, S. C.; Booth, P. J.; Templer, R. H. Estimations of lipid bilayer geometry in fluid lamellar phases. *Biochim. Biophys. Acta* **2000**, *1468*, 41−54.

(61) Nagle, J. F.; Wiener, M. C. Structure of Fully Hydrated Bilayer Dispersions. *Biochim. Biophys. Acta* **1988**, *942*, 1−10.

(62) Wiener, M. C.; Suter, R. M.; Nagle, J. F. Structure of the Fully Hydrated Gel Phase of Dipalmitoylphosphatidylcholine. *Biophys. J.* **1989**, *55*, 315−325.

$$\rho_{layer} = \phi_A\rho_A + \phi_B\rho_B + \phi_w\rho_w \quad (12)$$

By deuterating components A and B in turn or changing the water contrast, it is possible to define all three volume fractions of a mixed layer. In a simple surfactant or polyelectrolyte layer of uniform hydrophobicity, the solvent volume fraction is a direct measure of surface coverage. In a phospholipid bilayer, a further consideration arises from the different physical properties of the polar headgroup and nonpolar hydrocarbon chain regions, that is, the distribution of water across the bilayer is not uniform but even at 100% surface coverage there will be some water present in the headgroup regions if the requirement of a constant area per molecule is to be maintained. We, therefore, used the following constraint in all data fitting: The solvent in the bilayer must be distributed in such a way that, based on the relative volumes of the headgroup and chains, the area per molecule plus the associated water is constant across the bilayer, where by the associated water we mean the water content averaged over the entire area illuminated in the experiment (typically 65 × 30 mm^2).

In our three-layer bilayer model, consisting of the upper and lower (toward the silica surface) headgroup regions and a central hydrocarbon chain region, we assumed all layers could be modeled as noninterpenetrating homogeneous slabs. While each headgroup region was described by a separate layer, their properties were assumed to be identical and because of this constraint the number of independent layers in our model was only two. The thickness and solvent content of the most sensitive layer in a given contrast (e.g., hydrocarbon chains in D_2O or headgroups in chain-deuterated lipid) were modeled to give a coarse fit to the observed level of reflectivity, and the thickness and solvent fraction in the remaining regions were fitted keeping the area per molecule constant to within ±1 $Å^2$ across the bilayer. The fit was refined by adjusting the sublayer parameters while maintaining the stoichiometry until a satisfactory agreement with the data was reached. It was not necessary to incorporate any interfacial roughness into the bilayer model, nor was a solvent layer of the dimensions suggested previously[14] found to be present between the headgroups and the SiO_2 surface.

There are two types of fitting errors quoted in the tables of results. The errors in thickness, scattering length density, and volume fraction for any single sublayer are estimated from the maximum variation in the acceptable fit subject to the constraints of space filling and stoichiometry. However, because variations in sublayer structure are highly coupled in scattering length density, the resulting overall errors are only of the order of ±2 Å in bilayer thickness and ±2% in composition. The definition of an acceptable fit is necessarily somewhat subjective and depends on the experience of the user. Although χ^2 criteria are sometimes used to define fits, the combination of the nonlinearity of response of the reflectivity to structure and composition of the layer and the logarithmic variation of the reflectivity generally combine to render such criteria more or less useless. Here we display as many data and fits as are practicable, and the sensitivity and resolution of the experiment will be further discussed in Results.

4. Experimental Section

Ultrahigh-quality water (Ω = 18.2 Ω; Elga) was used in all experiments. D_2O for experiments at ISIS, U.K., was purchased from Sigma-Aldrich, and at ILL, Grenoble, it was provided from the reactor. Unlabeled DPPC, cholesterol, Tris-buffer, and β-D-dodecyl maltoside were purchased from Sigma-Aldrich at 99% purity and used without further purification. Chain-deuterated d_{62}-DPPC was obtained from Larodan Fine Chemicals, Sweden. Chain-deuterated d_{25}-β-D-dodecyl maltoside was synthesized in our laboratory as described by Hines et al.[31]

The solid supports for neutron reflection were 50 × 125 × 25 mm^3 silicon single crystals cut to provide a surface along the (111) plane. These were polished in-house and cleaned for 15 min in a mixture of 1:4:5 $H_2O_2/H_2SO_4/H_2O$ at 80−85 °C, followed by ozonolysis.[63] This treatment leaves a natural oxide layer of 7−20 Å thickness and 3−5 Å roughness.

Neutron reflection experiments were carried out on the SURF reflectometer[64] at the ISIS facility of the Rutherford-Appleton Laboratory in Didcot, U.K., and on the D17 reflectometer[65] at the Institute Laue-Langevin in Grenoble, France. All measurements were done in the time-of-flight mode, using wavelengths of 0.5−6 Å on SURF and 2.2−19 Å on D17. The sample solution was contained in a Teflon trough clamped against the Si surface with hollow aluminum plates that allowed temperature equilibration by a circulating water bath to an accuracy of ±0.3 °C. The cell has an inlet and outlet allowing the change of contents without exposing the surface to air and a cavity for a magnetic flea for stirring the bulk solution during adsorption.

A typical experimental procedure for bilayer formation consists of the following stages: adsorption from a 6:1 (w/w) % mixture of β-D-dodecyl maltoside and the requisite phospholipid at a concentration of 0.114−0.141 g/L, followed by rinsing with D_2O, readsorption from 10 and 100 times more dilute solutions, each followed by rinsing, and finally, a change to a buffer solution of 10 mM Tris at pH 7.4. All manipulations were performed in situ in the neutron reflectometer, with the reflectivity being recorded at each stage after equilibrium had been reached at the surface, which took from 1.5 h during the first adsorption step to 15−30 min for the subsequent rinsing and adsorption steps. Prior to adsorption of surfactants, the $Si-SiO_2$ surface was characterized in D_2O to establish the structure of the native oxide layer, to be used as a reference in fitting the data.

5. Results

5.1. Adsorption of DPPC and β-D-Dodecyl Maltoside. The adsorption of DPPC was studied at three different contrasts (isotopic compositions). These were (i) with hydrogenated DDM in D_2O, (ii) with chain-deuterated d_{25}-DDM in D_2O, and (iii) with d_{62}-DPPC and hydrogenated DDM in water contrast matched to silicon (CmSi, sld = 2.07 × 10^{-6} $Å^{-2}$). All experiments were performed at 25 ± 0.3 °C, and the initial concentrations of 0.114−0.141 g/L were diluted by factors of 10 and 100 in all cases. In addition, the formation of a bilayer of the D-α-DPPC stereoisomer was investigated.

Figure 1 shows the neutron reflectivity profiles of DPPC bilayers at three different adsorption and rinsing stages in D_2O and the bilayer properties for L-α-DPPC−DDM and D-α-DPPC−DDM mixtures are summarized in Tables 2 and 3. The general changes in reflectivity at each concentration and after each rinsing are very similar for both isomers. The only difference, which can be seen from Tables 2 and 3, is that the thickening of the bilayer that occurs upon the removal of surfactant is less pronounced for the D-isomer.

The reflectivity profiles from L-α-DPPC−d_{25}-DDM bilayers are shown in Figure 2, and the corresponding results for d_{62}-DPPC−DDM in CmSi are shown in Figure 3. The scattering length density of d_{25}-DDM is 3.76 × 10^{-6} $Å^{-2}$, and in Figure 2 its removal appears as an increase in contrast as the bilayer is enriched in phospholipid. In

(63) Thirtle, P. N. *Neutron reflection from modified silicon surfaces.* D.Phil. Thesis, Oxford University, Oxford, 1999.
(64) Penfold, J. The Application of Specular Neutron Reflection to the Study of Surfaces and Interfaces. *Physica B* **1992**, *180*, 462−464.
(65) Cubitt, R.; Fragneto, G. D17: the new reflectometer at the ILL. *Appl. Phys. A* **2002**, *74*, S329−S331.

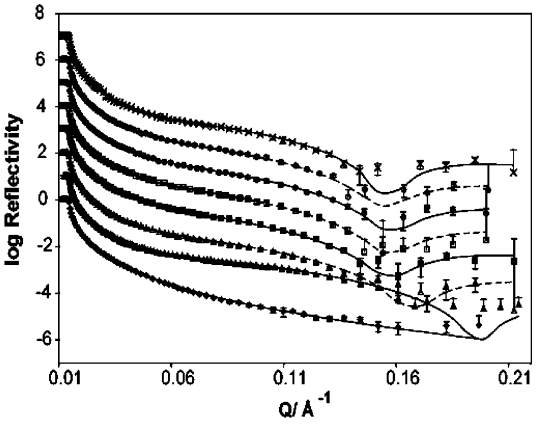

Figure 1. Reflectivity profiles recorded during adsorption of 1:6 L-α-DPPC−DDM mixtures on Si−SiO_2 in D_2O at 25 °C. (open diamonds) Substrate, (filled triangles) 10 × 0.114 g/L, (open triangles) 10^2 × D_2O rinse after 0.114 g/L, (filled squares) 10^3 × 0.0114 g/L, (open squares) 10^4 × D_2O rinse after 0.0114 g/L, (filled circles) 10^5 × 0.001 14 g/L, (open circles) 10^6 × D_2O rinse after 0.001 14 g/L, and (crosses) 10^7 × DPPC bilayer in 10 mM Tris-HCl at pH 7.4. The data sets have been displaced for clarity by successive factors of 10. The lines represent the reflectivity calculated using the parameters in Tables 1 and 2, and the markers indicate experimental data points. Error bars are shown on each reflectivity profile.

Figure 3, the reflectivity arises mainly from the chain-deuterated lipid, and the changes in contrast directly reflect the changes in the surface excess of DPPC. In both cases, the bilayer composition was found by comparing the fitted scattering length density of the hydrophobic chain region with that calculated for the phospholipid molecules, and the difference was used to estimate the volume fraction of DDM present. If no surfactant is present in the bilayer, the scattering length density of the chain region is given by eq 13:

$$\rho_{\text{layer}} = \phi_{\text{lipid}}\rho_{\text{lipid}} + (1 - \phi_{\text{lipid}})\rho_{\text{water}} \qquad (13)$$

If, however, some of the lipid chain region is occupied by the surfactant, this will change the apparent scattering length density of the layer:

$$\rho_{\text{layer}} = \phi_{\text{chains}}\rho_{\text{chains}} + \phi_{\text{water}}\rho_{\text{water}} \qquad (14)$$

In this case, the scattering length density of chains can be expressed as a sum of the phospholipid and surfactant:

$$\rho_{\text{chains}} = \phi_{\text{lipid}}\rho_{\text{lipid}} + \phi_{\text{DDM}}\rho_{\text{DDM}} \qquad (15)$$

The values of $\phi(d_{25}\text{-DDM})$ listed in Table 4 are the fractions of phospholipid volume occupied by the surfactant as defined in eq 15.

Bilayer properties derived from the fitted thickness and lipid volume fractions are presented in Tables 4 and 5. From the results it is obvious that most of the surfactant is removed in the first rinsing step and at lower concentrations the compositional changes are very small. Essentially, all the data sets fit to molecular areas between 55 and 70 Å^2, where the deviations arise from the variation in surface coverage (80 ± 10%, if 50 Å^2 per molecule is taken to be full coverage) between different experiments.

It can be seen in Figures 1 and 2 and in Tables 2 and 3 that the removal of surfactant is accompanied by an increase in bilayer thickness, indicating that the surfactant interferes with the packing of DPPC molecules. This is in contrast to our previous results on the coadsorption of DOPC and POPC with DDM, where no such dramatic thickening effect is seen. That this thickening effect is not apparent in the partially deuterated bilayers (Tables 4 and 5 and Figures 2 and 3) may be related to a difficulty in assigning the precise headgroup−chain region interface in the cases where either phospholipid or surfactant is chain-deuterated.

The D-α-DPPC bilayer is also somewhat thinner than the L-α-DPPC bilayer, indicating poorer lipid packing of the D-isomer. This may be due either to contamination of the sample by small amounts of the L-isomer, which would disturb the packing, or due to a stronger interaction of the D-isomer with β-DDM. α-DDM has been reported to be a much poorer solubilizing agent for L-α-phospholipids,[66] and it is probable that the phospholipid stereochemistry is important in determining the interactions in a mixed bilayer. A deuterated D-DPPC isomer would, however, be required to resolve this question with any certainty.

Performing the micellar adsorption at 37 °C was found to lead to a significantly reduced surface coverage, which was taken to be a consequence of the increased solubility of the DPPC−DDM mixture at the higher temperature. However, bilayer formation at 25 °C was very reproducible and rapid (∼3−3.5 h in total excluding the neutron measurement time), and once all surfactant had been removed from the sample cell, we found the bilayers to be stable to heating to 37 °C.

5.2. Adsorption of DPPC and Cholesterol with β-D-Dodecyl Maltoside. We also examined the applicability of micellar adsorption to a ternary mixture of β-DDM, DPPC, and cholesterol, where the surfactant-to-lipid ratio was 6:1, but with 10% of the lipid weight replaced by cholesterol. Using d_{62}-DPPC−DDM and d_{25}-DDM in D_2O allowed us to monitor the cholesterol adsorption and to determine the location of cholesterol normal to the interface. The reflectivity profiles in D_2O are shown in Figure 4, where the small changes in contrast arise mainly from the changes in the bilayer cholesterol content and in the hydration of the lipid headgroups. To model the mixed DPPC−cholesterol bilayer, we used a model in which additional coupled slabs on both sides of the bilayer describe the location of cholesterol in the DPPC chain region, but from fitting the thickness of this region leads to a cholesterol-free region in the center of the bilayer. Hence, the number of independent boxes used was three, that is, headgroups, chain/cholesterol, and chains. The results in Table 6 show that there is an initial adsorption of cholesterol at a volume fraction of 17% (of the lipid volume) but that this gradually decreases with decreasing bulk concentration to 13%. This volume fraction corresponds to 14 wt % or 26 mol %, indicating that overall the adsorption of cholesterol is enhanced by using a micellar lipid−surfactant mixture. The bilayer structure referred to in Table 6 is illustrated in Figure 5, where the location of a cholesterol molecule relative to DPPC is shown. The volume fractions of cholesterol in Table 6 correspond to the volume fraction of lipid chains displaced. There appears to be a condensation of the lipid upon exchange of the last lipid−surfactant solution (in D_2O) to a Tris buffer solution in CmSi. While this may be an isotope effect, it is more likely the result of the higher sensitivity of the CmSi contrast to the (deuterated) phospholipid properties. It is also possible that some additional DPPC adsorption has in fact occurred during the slow exchange of solutions. The properties of cholesterol, however, agree very well within the two contrasts.

(66) Caussanel, F.; Andre-Barres, C.; Lesieur, S.; Rico-Lattes, I. A comparative study of sugar-based surfactants for the solubilization of phosphatidylcholine vesicles. *Colloids Surf., B* **2001**, *22*, 193−203.

Table 2. Fitted Parameters and Calculated Properties of L-α-DPPC−DDM Mixtures

concentration	layer	$\rho_a/10^{-6}$ Å^{-2}	d/Å	ϕ	A_a/Å^2	Γ/mg m^{-2}
0.114 g/L[a]	head	2.9 ± 0.2	6 ± 1	0.76 ± 0.05	72 ± 7	3.4 ± 0.3
	chains	0.4 ± 0.1	28 ± 2	0.89 ± 0.02	71 ± 7	
D_2O rinse	head	3.3 ± 0.2	7 ± 1	0.67 ± 0.05	70 ± 7	3.5 ± 0.3
	chains	1.5 ± 0.2	35 ± 2	0.73 ± 0.02	70 ± 7	
0.0114 g/L	head	3.1 ± 0.2	7 ± 1	0.72 ± 0.05	65 ± 7	3.8 ± 0.4
	chains	1.4 ± 0.1	37 ± 2	0.74 ± 0.02	65 ± 7	
D_2O rinse	head	3.1 ± 0.2	7 ± 1	0.72 ± 0.05	65 ± 7	3.8 ± 0.4
	chains	1.4 ± 0.1	37 ± 2	0.74 ± 0.02	65 ± 7	
0.001 14 g/L	head	3.2 ± 0.2	7 ± 1	0.70 ± 0.05	67 ± 7	3.7 ± 0.4
	chains	1.5 ± 0.1	37 ± 2	0.72 ± 0.02	67 ± 7	
D_2O rinse	head	3.2 ± 0.2	7 ± 1	0.70 ± 0.05	67 ± 7	3.7 ± 0.4
	chains	1.6 ± 0.1	38 ± 2	0.70 ± 0.02	67 ± 7	
pH 7.35 D_2O	head	3.7 ± 0.2	8 ± 1	0.59 ± 0.05	69 ± 7	3.5 ± 0.4
in 10 mM Tris−HCl	chains	1.8 ± 0.1	38 ± 2	0.67 ± 0.02	70 ± 7	

[a] A 3 Å layer of D_2O was fitted between the substrate and lipid headgroups. ρ_α denotes the scattering length density of layer a including solvent, corresponding to a volume fraction ϕ of the lipid, assumed to have a molecular scattering length density ρ as indicated in Table 1.

Table 3. Fitted Parameters and Calculated Properties of D-α-DPPC−DDM Bilayers[a]

concentration	layer	$\rho_a/10^{-6}$ Å^{-2}	d/Å	ϕ	A_a/Å^2	Γ/mg m^{-2}
0.114 g/L	head	3.1 ± 0.2	6 ± 1	0.72 ± 0.05	76 ± 8	3.3 ± 0.3
	chains	0.3 ± 0.1	27 ± 2	0.90 ± 0.02	73 ± 7	
D_2O rinse	head	4.1 ± 0.2	8 ± 1	0.50 ± 0.05	82 ± 8	3.0 ± 0.3
	chains	1.6 ± 0.1	31 ± 2	0.70 ± 0.02	82 ± 8	
0.0114 g/L	head	3.6 ± 0.2	8 ± 1	0.62 ± 0.05	66 ± 7	3.7 ± 0.4
	chains	0.8 ± 0.1	33 ± 2	0.82 ± 0.02	66 ± 7	
D_2O rinse	head	3.5 ± 0.2	8 ± 1	0.63 ± 0.05	65 ± 7	3.8 ± 0.4
	chains	0.6 ± 0.1	32 ± 2	0.86 ± 0.02	65 ± 7	
0.001 14 g/L	head	3.6 ± 0.2	8 ± 1	0.62 ± 0.05	66 ± 7	3.7 ± 0.4
	chains	1.0 ± 0.1	34 ± 2	0.80 ± 0.02	65 ± 7	
pH 7.35 D_2O	head	3.6 ± 0.2	8 ± 1	0.62 ± 0.05	66 ± 7	3.7 ± 0.4
10 mM Tris−HCl	chains	0.9 ± 0.1	33 ± 2	0.82 ± 0.02	66 ± 7	

[a] ρ_α denotes the scattering length density of layer a including solvent, corresponding to a volume fraction ϕ of the lipid, assumed to have a molecular scattering length density ρ as indicated in Table 1.

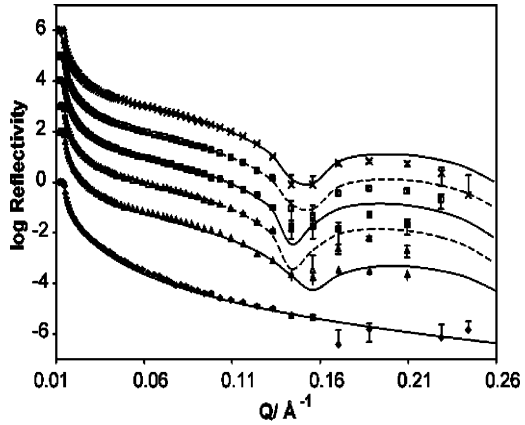

Figure 2. Reflectivity profiles recorded during adsorption of 1:6 L-α-d_{25}-DPPC−DDM mixtures on Si−SiO_2 in D_2O at 25 °C. (open diamonds) Substrate, (filled triangles) $10^2 \times$ 0.114 g/L, (open triangles) $10^3 \times$ D_2O rinse after 0.114 g/L, (filled squares) $10^4 \times$ 0.0114 g/L, (open squares) $10^5 \times$ D_2O rinse after 0.0114 g/L, and (crosses) $10^6 \times$ DPPC bilayer after D_2O rinse after 0.001 14 g/L in 10 mM Tris-HCl at pH 7.4. The lines represent the reflectivity calculated using the parameters in Tables 1 and 4, and the markers indicate experimental data points. Representative error bars are shown on the substrate reflectivity profile.

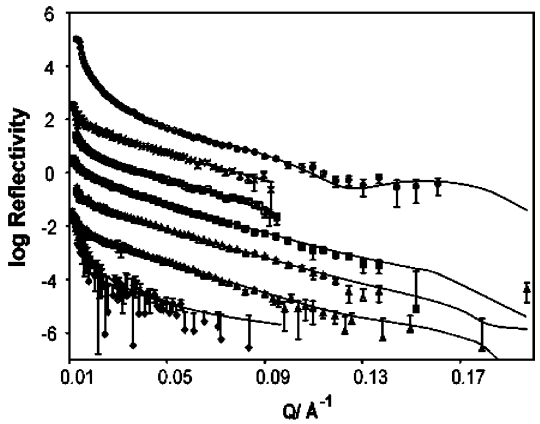

Figure 3. Reflectivity profiles recorded during adsorption of 1:6 d_{62}-DPPC−DDM mixtures in CmSi on Si−SiO_2 at 25 °C. (open diamonds) Substrate, (filled triangles) 10 × 0.114 g/L, (open triangles) $10^2 \times$ CmSi rinse after 0.114 g/L, (filled squares) $10^3 \times$ 0.0114 g/L, (open squares) $10^4 \times$ CmSi rinse after 0.0114 g/L, (open circles) $10^5 \times$ D_2O rinse after 0.001 14 g/L, and (crosses) $10^6 \times$ DPPC bilayer in 10 mM Tris-CmSi at pH 7.4. The lines represent the reflectivity calculated using the parameters in Tables 1 and 5, and the markers indicate experimental data points. Error bars are shown on each reflectivity profile.

The mean location of cholesterol is found to be directly below the DPPC headgroup region, extending 18 ± 1 Å into the hydrophobic chain region on both sides of the bilayer, with a cholesterol-free region of 8 ± 1 Å in the center of the bilayer. This location correlates well with that found for cholesterol by neutron diffraction from stacks of bilayers,[67] which showed that the OH group of cholesterol is located in the lipid acyl group region. There is a 4 ± 1 Å interfacial roughness that propagates throughout the DPPC−cholesterol bilayer, which was not observed in the absence of cholesterol. Possible reasons for this roughening effect are indicated in Discussion. The

(67) Worcester, D. L.; Franks, N. P. Structural Analysis of Hydrated Egg Lecithin and Cholesterol Bilayers. *J. Mol. Biol.* **1976**, *100*, 359−378.

Table 4. Results for the Adsorption of L-α-DPPC−d_{25}-DDM Mixtures in D_2O[a]

concentration	layer	$\rho/10^{-6}$ Å^{-2}	$\rho_a/10^{-6}$ Å^{-2}	$\phi(d_{25}$-DDM)	d/Å	ϕ	A/Å^2	Γ/mg m^{-2}
0.123 g/L	head	1.84	2.7 ± 0.1	0.1 ± 0.01	7 ± 1	0.8 ± 0.05	58 ± 6	4.5 ± 0.5
	chains	0.34	0.9 ± 0.05	0.1 ± 0.01	34 ± 2	0.9 ± 0.02	58 ± 6	
D_2O rinse	head	1.84	2.8 ± 0.1		7 ± 1	0.78 ± 0.05	60 ± 6	4.4 ± 0.4
	chains	−0.36	−0.3 ± 0.05		33 ± 2	0.9 ± 0.02	60 ± 6	
0.0123 g/L	head	1.84	2.7 ± 0.1		7 ± 1	0.8 ± 0.05	58 ± 6	4.5 ± 0.5
	chains	−0.36	−0.3 ± 0.05		34 ± 2	0.9 ± 0.02	58 ± 6	
D_2O rinse	head	1.84	2.4 ± 0.1		7 ± 1	0.87 ± 0.05	54 ± 5	4.9 ± 0.5
	chains	−0.36	−0.25 ± 0.05		35 ± 2	0.95 ± 0.02	54 ± 5	
pH 8 D_2O[b]	head	1.84	2.4 ± 0.1		7 ± 1	0.88 ± 0.05	53 ± 5	4.9 ± 0.5
10 mM Tris−HCl	chains	−0.36	−0.17 ± 0.05		35 ± 2	0.97 ± 0.02	52 ± 5	

[a] ρ denotes the molecular scattering length density calculated from phospholipid volumes and scattering lengths as given in Table 1. The amount of surfactant, $\phi(d_{25}$-DDM), was calculated from the difference found between the fitted and the calculated values of ρ for the hydrophobic chain region. [b] In 2 mM $CaCl_2$.

Table 5. Adsorption of d_{62}-L-α-DPPC−DDM Mixtures in CmSi

concentration	layer	$\rho/10^{-6}$ Å^{-2}	$\rho_a/10^{-6}$ Å^{-2}	$\phi(d_{25}$-DDM)	d/Å	ϕ	A_a/Å^2	Γ/mg m^{-2}
d_{62}-DPPC−DDM	head	1.84	2.0 ± 0.1	0.26 ± 0.01	7 ± 1	0.49 ± 0.05	95 ± 26	2.6 ± 0.4
0.114 g/L	chains	5.00	3.8 ± 0.1	0.26 ± 0.01	38 ± 2	0.49 ± 0.02	95 ± 9	
CmSi rinse	head	1.84	1.9 ± 0.1		7 ± 1	0.65 ± 0.05	72 ± 18	3.4 ± 0.5
	chains	6.89	5.2 ± 0.1		38 ± 2	0.65 ± 0.02	72 ± 6	
d_{62}-DPPC−DDM	head	1.84	1.9 ± 0.1		7 ± 1	0.59 ± 0.05	76 ± 19	3.2 ± 0.5
0.0114 g/L	chains	6.89	5.0 ± 0.1		38 ± 2	0.59 ± 0.02	77 ± 7	
CmSi rinse	head	1.84	1.9 ± 0.1		7 ± 1	0.59 ± 0.05	76 ± 19	3.2 ± 0.5
	chains	6.89	5.0 ± 0.1		38 ± 2	0.59 ± 0.02	77 ± 7	
d_{62}-DPPC[a]	head	1.84	3.7 ± 0.2		7 ± 1	0.61 ± 0.05	76 ± 19	3.2 ± 0.5
D_2O pH 7.4	chains	6.89	5.0 ± 0.1		38 ± 2	0.61 ± 0.02	77 ± 7	

[a] A 5 Å layer of D_2O was fitted between the substrate and the lipid headgroups.

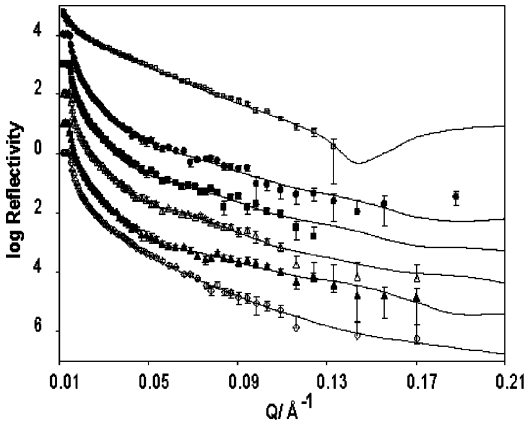

Figure 4. Reflectivity profiles recorded during adsorption of 1:6 L-α-d_{62}-DPP−d_{25}-DDM−cholesterol mixtures on Si−SiO_2 in D_2O at 25 °C. (open diamonds) Substrate, (filled triangles) 10 × 0.141 g/L, (open triangles) 10^2 × D_2O rinse after 0.141 g/L, (filled squares) 10^3 × 0.0141 g/L, (filled circles) 10^4 × 0.001 41 g/L, and (open circles) 10^6 × DPPC−cholesterol bilayer in 10 mM CmSi Tris-HCl at pH 7.4. The data sets have been displaced by successive factors of 10 for clarity. The lines represent the reflectivity calculated using the parameters in Tables 1 and 6, and the markers indicate experimental data points. Error bars are shown on each reflectivity profile.

presence of this roughness also leads to higher thickness values of the hydrophobic region than would be expected for DPPC, for which the all-trans chain length is 18 Å.

6. Discussion

We have shown that β-D-dodecyl maltoside can be used as an efficient solubilizing agent in the deposition of phospholipids and that high-quality DPPC bilayers are formed via this process. The structures determined for our DPPC bilayers are in relatively good agreement with those for DPPC bilayers formed by Langmuir−Shaeffer deposition[18] or adsorption of small unilamellar vesicles,[15] but we did not find it necessary to include either interfacial roughness into the bilayer models or to include a solvent layer of the dimensions suggested by Johnson et al.[14] between the bilayer and the silicon support. Only a 3 ± 2 Å layer of solvent was present, which we attribute to some porosity in the SiO_2 surface on a lateral scale too small to incorporate lipid headgroups. The most likely reason for the thick water layer observed by Johnson et al. would seem to be an SiO_2 gel layer of high D_2O content, which readily formed by quartz under alkaline conditions but not at a Si(111) surface which only has a thin native oxide layer.[68]

The structure determination of neutron reflectivity is based on measuring the scattering length averaged over the entire illuminated area; hence, it is only possible to determine the average area available per phospholipid molecule on the surface, and it should be noted that this does not correspond to the actual volume occupied by each individual molecule. The molecular areas listed in the tables of results are derived from the hydrophobic and polar region thicknesses and scattering length densities assuming that the molecules have the dimensions listed in Table 1. In a situation when the surface coverage is incomplete, we envisage, as has also been found to be the case by atomic force microscopy,[69] that the phospholipids occupy the surface in islands or as a continuous bilayer with defects. The lateral arrangement in such cases is known to be dependent on the lipid chain melting temperature, that is, that lipids in a fluid bilayer are to some extent able to accommodate larger molecular areas by spreading uniformly over the available area, whereas lipids below their melting point spread less readily. In using neutron reflection, the main point of our focus has been to determine the chemical composition of the bilayers.

(68) Iler, R. K. *The Chemistry of Silica*; John Wiley & Sons: New York, 1979.

(69) Leonenko, Z. V.; Carnini, A.; Cramb, D. T. Supported planar bilayer formation by vesicle fusion: the interaction of phospholipid vesicles with surfaces and the effect of gramicidin on bilayer properties using atomic force microscopy. *Biochim. Biophys. Acta* **2000**, *1509*, 131−147.

Table 6. Results from the Adsorption of d_{62}-L-α-DPPC−d_{25}-DDM−10 (w/w) % Cholesterol

concentration	layer	$\rho_a/10^{-6}$ Å^{-2}	d/Å	ϕ	A/Å^2	Γ/mg m^{-2}
0.141 g/L[a]	head	3.7 ± 0.1	7 ± 1	0.59 ± 0.05	79 ± 8	3.1 ± 0.3
	chains	6.7 ± 0.7	38 ± 2	0.59 ± 0.1	79 ± 8	
	cholesterol[b]	5.3 ± 0.1	16 ± 1	0.23 ± 0.02	164 ± 16	0.8 ± 0.1
D_2O rinse[a]	head	3.3 ± 0.1	8 ± 1	0.54 ± 0.05	76 ± 8	3.2 ± 0.3
	chains	6.3 ± 0.6	42 ± 2	0.56 ± 0.1	76 ± 8	
	cholesterol	5.7 ± 0.4	18 ± 1	0.14 ± 0.02	239 ± 24	0.5 ± 0.1
0.0141 g/L[a]	head	3.2 ± 0.1	8 ± 1	0.56 ± 0.05	73 ± 7	3.3 ± 0.3
	chains	6.2 ± 0.6	42 ± 2	0.58 ± 0.1	73 ± 7	
	cholesterol	5.9 ± 0.5	18 ± 1	0.17 ± 0.02	197 ± 20	0.6 ± 0.1
0.001 41 g/L[a]	head	3.8 ± 0.1	8 ± 1	0.56 ± 0.05	73 ± 7	3.3 ± 0.3
	chains	6.7 ± 0.7	42 ± 2	0.58 ± 0.1	73 ± 7	
	cholesterol	5.9 ± 0.4	18 ± 1	0.15 ± 0.02	223 ± 22	0.6 ± 0.1
CmSi	head	1.9 ± 0.2	9 ± 1	0.73 ± 0.05	50 ± 15	5.0 ± 0.5
10 mM Tris-HCl	chains	5.0 ± 0.7	50 ± 2	0.73 ± 0.1	49 ± 3	
pH 7.4	cholesterol	5.6 ± 0.4	19 ± 1	0.73 ± 0.02	243 ± 60	0.5 ± 0.1

[a] The bilayer had an interfacial roughness of 4 Å throughout the sublayers. [b] The location of cholesterol in the bilayer is illustrated in Figure 5. ρ_a describes the total scattering length density of each layer including the solvent. The fitted values of ρ, the sum of molecular scattering length densities (listed in Table 1) used to describe the mixed system for each layer, are illustrated in Figure 5. The volume fraction and area per cholesterol molecule were calculated from the scattering length density of the region containing cholesterol and lipid.

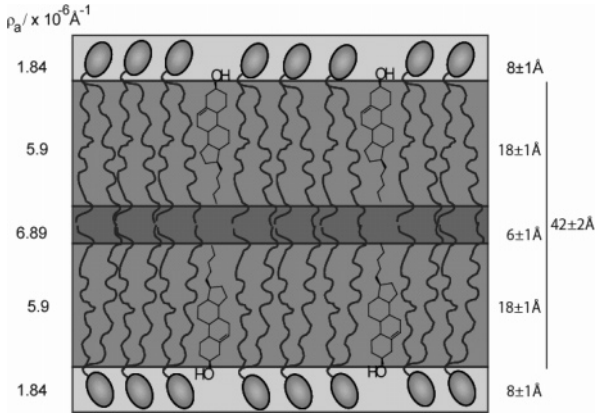

Figure 5. Box model of the vertical distribution of cholesterol relative to DPPC used for fitting d_{62}-DPPC−10%-cholesterol−d_{25}-DDM data. The scattering length densities indicated are those fitted for the mixed system (and do not include the solvent), where 1.84 and 6.89 × 10^{-6} Å^{-2} correspond to pure DPPC headgroups and chains, respectively, and the value 5.9 × 10^{-6} Å^{-2} was fitted to describe the amount of cholesterol in the mixed region. Cholesterol is located below the lipid headgroups on both sides of the bilayer but does not extend to the center of the bilayer, where a cholesterol-free layer of 6−8 Å exists depending on cholesterol content.

The elimination of β-D-dodecyl maltoside from the bilayer via rinsing has previously been demonstrated in DOPC bilayers,[23] but the DPPC−β-D-dodecyl maltoside exhibits markedly different behavior. In the fluid DOPC bilayer, the washing out of the surfactant is a gradual process which requires copious quantities of water, whereas all the surfactant is removed from the DPPC bilayer in the first rinsing step. This indicates that the interaction between the surfactant and DPPC is less favorable and that there may even be a miscibility transition below which the surfactant is expelled. The thickening of the DPPC bilayers that occurs concomitantly with the surfactant expulsion may be a further indication that, at high concentrations, the surfactant severely disturbs the packing of DPPC by causing either interdigitation of the layers or more likely significant tilting to accommodate the large sugar headgroups. As the amount of surfactant decreases, the bilayer adopts a more ordered structure from which the surfactant is squeezed out. The sensitivity of neutron reflectivity to the presence of the surfactant is of the order of 2 vol %, which gives rise to a difference in the phospholipid scattering length density of 0.15 × 10^{-6} Å^{-2}. The corresponding molar fraction of 3%, that is, 1.5% in each monolayer, is of the same order of magnitude as that typically used when adding fluorescence probes into lipid monolayers without their presence altering the monolayer structure or properties.[70]

In all cases it is evident that our supported bilayers appear to have larger areas per molecule and are more hydrated than the bulk lamellar phases of DPPC. We attribute this difference to the fact that the supported bilayer is also restricted by an interaction with the silica surface, while lacking the inter-bilayer interaction present in the bulk phase. Both interactions are electrostatic in nature, but the interaction between a negatively charged surface and a phosphatidylcholine has to be attractive for the surface layer to be stable, whereas in the bulk, the headgroup repulsion leads to an equilibrium water layer thickness between bilayers. We believe that this difference in the nature of headgroup interactions explains the lack of a thick water layer between the headgroups and the surface. The support is a macroscopic surface of an area of 5000 mm^2, and as such is likely to have defects, which may lead to an incomplete surface coverage. The larger water contents observed in supported bilayers are a result of the averaging nature of the neutron experiment, which yields the total amount of water in the bilayer but not its lateral distribution. The structure of an incomplete DPPC bilayer at 25 °C is likely to be a network of islands, in contrast to a more continuous bilayer formed by lipids in the fluid phase which spread more readily. On the contrary, reflectivity is very sensitive to the vertical distribution of water across the bilayer, and we find that, despite the surface defects, there is generally an ∼10% larger hydration of the headgroups compared to the chains. The water content of the headgroup relative to the chain region is a reflection of the relative volumes and lengths of the lipid headgroups and chains. A larger thickness of the headgroup region would require a higher degree of hydration to maintain the molecular stoichiometry in the bilayer.

The choice of which molecular scattering lengths to use to derive molecular properties from a neutron reflectivity measurement is to some extent as arbitrary as the division of the layer into polar and nonpolar regions. It is, however, possible to show that the requirement of a constant molecular area across the bilayer puts some bounds on the choice of division. If the molecular volume is ill-divided, it can lead to a situation where it is impossible to distribute

(70) Moore, B.; Knobler, C. M.; Broseta, D.; Rondelez, F. *J. Chem. Soc., Faraday Trans. I* **1986**, *82*, 1753.

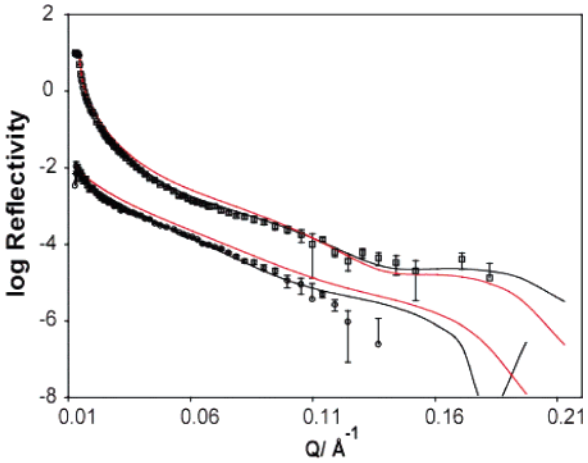

Figure 6. Reflectivity of a single d_{62}-DPPC bilayer: 10× in D_2O (open squares) and in CmSi (open circles). The black lines represent a fit using the parameters in Table 5. The red lines are the reflectivities calculated using 7.74×10^{-6} Å^{-2} as the DPPC chain scattering length density.

the lipid and water in a physically meaningful way while maintaining the molecular area constant. Previously, Koenig et al.[15] have reported difficulties in deriving detailed structural information from reflectivity data on DPPC bilayers, which were modeled using molecular volumes from X-ray crystallographic and densitometric measurements of DPPC at 20 °C.[62,71] They interpreted the headgroup thicknesses of 11−15 Å and the resulting unphysical scattering length densities as arising from a rippled structure, although there was no direct evidence for such a structure. The determination of the molecular distribution for a rippled structure would indeed be difficult. Their values for the headgroup scattering length densities were in some cases observed to be higher than either that for the phospholipid headgroup or that for the solvent. Because this is physically impossible it indicates a problem in the division between the headgroup and the (deuterated) chain regions. In the case of hydrogenated DPPC, a 100 Å^3 difference in hydrocarbon chain volume only gives rise to a 0.04×10^{-6} Å^{-2} difference in scattering length densities, which is within the error limits of our data fitting. For chain-deuterated DPPC, however, crystalline chain packing as assumed by Koenig et al. would give rise to a chain scattering length density of 7.74×10^{-6} Å^{-2} as opposed to our value of 6.89×10^{-6} Å^{-2}. Figure 6 shows the reflectivity of the same d_{62}-DPPC bilayer recorded in CmSi and D_2O, with data fits based on our data analysis shown in black. The red lines indicate what the reflectivity would be if the scattering length density of DPPC chains is taken to be 7.74×10^{-6} Å^{-1}. From these data, we actually found that it is only possible to obtain an acceptable fit using the value of 7.74×10^{-6} Å^{-2} in the unphysical situation where there is more water in the hydrocarbon core of the bilayer than in the headgroup region. Our lower scattering length density for the chain region supports the idea that the phospholipid packing is disturbed by the headgroup−surface interactions, making a supported bilayer more disordered than a bulk lamellar phase and perhaps more akin to the biological cell membrane which is a disordered, fluid structure with a high degree of lateral heterogeneity and contacts the supporting network of the cytoskeleton.

The coadsorption of cholesterol in mixed DPPC−surfactant micelles leads to its successful incorporation into the resulting bilayer, in a manner that shows a slight dependence on bulk concentration. This indicates that deposition from micellar solutions of more complex mixtures can follow the same principles as that from binary surfactant mixtures, that is, that both the overall concentration and relative hydrophobicity of the components govern the composition of adsorbed layers. Cholesterol is found to reside in an 18 ± 1 Å thick layer immediately adjacent to the lipid headgroup region on both sides of the supported bilayer, which is consistent with molecular simulations on cholesterol-containing DPPC and other phospholipid bilayers.[72−76] The presence of cholesterol leads to a bilayer roughness of 4 ± 1 Å, which was not observed for pure DPPC bilayers. A 4 Å increase in the thickness of the hydrophobic region is observed in the presence of cholesterol, and this correlates well with the 3.5 Å increase in the thickness of a DMPC bilayer measured in a neutron diffraction study,[77] which also locates ring A of cholesterol immediately below the headgroup region and at 15.5 Å from the bilayer center but does not resolve the thickness of the region occupied by the entire molecule. Quasi-elastic neutron scattering has been used to determine that in DPPC bilayers cholesterol exhibits both rotational in-plane motion as well as out-of-plane diffusion in the direction of the bilayer normal at temperatures above 36 °C but that this motion is largely frozen out at 20 °C.[78] The thickness of 18 Å of the cholesterol-containing region is smaller than the all-trans length of a cholesterol molecule (22 Å), indicating the presence of some gauche bonds in the cholesterol chain. While the length scale of the observed bilayer roughness is of the same magnitude as the out-of-plane diffusional motion measured by Gliss et al., our results do not support their conclusion that this motion occurs toward the bilayer core, because an 8 Å thick cholesterol free region is found at the center.

The role of cholesterol in lipid bilayers has been widely investigated, and it is known to broaden the gel-to-liquid-crystalline phase transition in bulk lamellar phases.[79] In our case, at a molecular ratio of four lipids per cholesterol, its effect appears to be to disturb the packing to DPPC chains in a way that leads to a 4 Å roughening of the bilayer accompanied by a significant increase in the bilayer

(71) Nagle, J. F.; Wilkinson, D. A. Lecithin Bilayers: Density Measurements and Molecular Interactions. *Biophys. J.* **1978**, *23*, 159−175.

(72) Smondyrev, A. M.; Berkowitz, M. L. Structure of dipalmitoylphosphatidylcholine/cholesterol bilayer at low and high cholesterol concentrations: Molecular dynamics simulation. *Biophys. J.* **1999**, *77*, 2075−2089.

(73) Pasenkiewicz-Gierula, M.; Rog, T.; Kitamura, K.; Kusumi, A. Cholesterol effects on the phosphatidylcholine bilayer polar region: A molecular simulation study. *Biophys. J.* **2000**, *78*, 1376−1389.

(74) Chiu, S. W.; Jakobsson, E.; Mashl, R. J.; Scott, H. L. Cholesterol-induced modifications in lipid bilayers: A simulation study. *Biophys. J.* **2002**, *83*, 1842−1853.

(75) Hofsass, C.; Lindahl, E.; Edholm, O. Molecular dynamics simulations of phospholipid bilayers with cholesterol. *Biophys. J.* **2003**, *84*, 2192−2206.

(76) Tu, K. C.; Klein, M. L.; Tobias, D. J. Constant-pressure molecular dynamics investigation of cholesterol effects in a dipalmitoylphosphatidylcholine bilayer. *Biophys. J.* **1998**, *75*, 2147−2156.

(77) Leonard, A.; Escrive, C.; Laguerre, M.; Pebay-Peyroula, E.; Neri, W.; Pott, T.; Katsaras, J.; Dufourc, E. J. Location of cholesterol in DMPC membranes. A comparative study by neutron diffraction and molecular mechanics simulation. *Langmuir* **2001**, *17*, 2019−2030.

(78) Gliss, C.; Randel, O.; Casalta, H.; Sackmann, E.; Zorn, R.; Bayerl, T. Anisotropic motion of cholesterol in oriented DPPC bilayers studied by quasielastic neutron scattering: The liquid-ordered phase. *Biophys. J.* **1999**, *77*, 331−340.

(79) McMullen, T. P. W.; McElhaney, R. N. Physical studies of cholesterol-phospholipid interactions. *Curr. Opin. Colloid Interface Sci.* **1996**, *1*, 83−90.

thickness. This could be a result of the planar supported bilayer compensating for the poorer packing of headgroups due to the rigid cholesterol molecules in the chain region leading to sliding of the DPPC molecules along their axes and a smearing out of the interfaces. Alternatively, this could be the average result of domain formation upon phase separation of the mixture into cholesterol-rich and DPPC-rich regions of different thicknesses, which would appear as an interfacial roughness in the absence of coherent off-specular scattering from the domains. Deuterium NMR studies of phospholipid−cholesterol bilayers indicate that the presence of large amounts of cholesterol induces a glassy arrangement in which the lateral diffusion of the lipids is restricted by the rigid cholesterol molecules, but unlike in an L_β gel phase, the molecules do not exhibit lateral ordering onto specific lattice sites.[80]

Although neutron reflection does not have the resolution to detect the lateral arrangement of molecules in a bilayer, it offers a compositional insight into how the presence of cholesterol, even at low concentrations, alters the structure of supported membranes, and as a result of the simple reflection geometry, both the amount and location of cholesterol can be determined simultaneously. The reflectivity results show sensitivity to ±2% in the cholesterol volume fraction in a chain-deuterated bilayer, indicating that neutron reflection could be used as a powerful tool for further investigations of the composition of mixed bilayers.

Acknowledgment. We thank the UK Engineering and Physical Sciences Research Council (EPSRC), the Biotechnology and Biological Sciences Research Council (BBSRC), the Academy of Finland, and the Finnish Cultural Foundation for their financial support and R. Cubitt (ILL), J. Webster, and S. Holt (ISIS) for assistance with the neutron reflection experiments.

LA047389E

(80) Huang, T. H.; Lee, C. W. B.; Das Gupta, S. K.; Blume, A.; Griffin, R. G. A Carbon-13 and Deuterium Nuclear Magnetic Resonance Study of Phosphatidylcholine/Cholesterol Interactions: Characterization of Liquid-Gel Phases. *Biochemistry* **1993**, *32*, 13277−13287.

(81) Petrache, H. I.; Feller, S. E.; Nagle, J. F. Determination of component volumes of lipid bilayers from simulations. *Biophys. J.* **1997**, *72*, 2237−2242.

(82) Weast, R. J., Ed. *Handbook of Chemistry and Physics*, 54th ed.; CRC Press: Cleveland, OH, 1973.